Desalination and Water Treatment
www.deswater.com

doi:10.5004/dwt.2018.22238

111 (2018) 310–321
April

Efficient adsorption of cobalt on chemical modified activated carbon: characterization, optimization and modeling studies

Babak Kakavandi[a,b], Alireza Raofi[c], Seyed Mohsen Peyghambarzadeh[c], Bahman Ramavandi[d], Maryam Hazrati Niri[b,e], Mehdi Ahmadi[b,e,*]

[a]*Research Center for Health, Safety and Environment, Alborz University of Medical Sciences, Karaj, Iran, email: kakavandibvch@gmail.com (B. Kakavandi)*
[b]*Department of Environmental Health Engineering, Alborz University of Medical Sciences, Karaj, Iran, email: Maryam_n@yahoo.com (M.H. Niri), Tel. +98 912 677 9273, email: ahmadi241@gmail.com (M. Ahmadi)*
[c]*Department of Chemical Engineering, Mahshahr Branch, Islamic Azad University, Mahshahr, Iran, email: alireza_raoofi@ymail.com (A. Raofi), peyghambarzadeh@gmail.com (S.M. Peyghambarzadeh)*
[d]*Department of Environmental Health Engineering, Bushehr University of Medical Sciences, Bushehr, Iran, email: ramavandi_b@yahoo.com (B. Ramavandi)*
[e]*Environmental Technologies Research Center, Ahvaz Jundishapur University of Medical Sciences, Ahvaz, Iran*

Received 11 November 2017; Accepted 24 March 2018

ABSTRACT

Herein, granular activated carbon (GAC) was modified chemically with sodium dodecyl sulfate (SDS) to prepare MGAC as an efficient adsorbent for removal of Co(II) ion from aqueous solution. The effect of different SDS concentrations and modification time on the adsorption performance was examined. The as-prepared adsorbent was characterized by FESEM and FT-IR techniques. Moreover, some parameters affecting the adsorption efficiency like solution pH, contact time, adsorbent dosages, initial metal ion concentrations, temperature and agitation speed on the adsorption efficiency were evaluated in a batch environment. Under same operational conditions, MGAC showed a much greater adsorption rate than GAC, due to synergistic effect between GAC and SDS. The equilibrium time was 90 min and the maximum adsorption capacity based on the Langmuir was found to be 51 mg/g. Experimental data were in good agreement with Langmuir and pseudo-second-order models. The mechanism of Co ion adsorption on MGAC followed ion-exchange and mono layer chemical adsorption. The adsorption process showed better performance at neutral pH and higher temperatures. Under optimized conditions, complete removal of 20 mg/L of Co(II) was obtained in the presence of 1.2 g/L of MGAC. Thermodynamic studies indicated the adsorption process was endothermic and spontaneous in nature.

Keywords: Adsorption; Activated carbon; Chemical modification; Heavy metal; Surfactant

1. Introduction

Development of industrial activities and consequently increasing discharging contaminants from industries have undesirably affected both environmental resources and human health. Heavy metals have been known as highly toxic and hazardous elements which are main proportion of contaminants end up to the soil and water resources by these activities [1,2]. Heavy metals can be found in high concentrations in industrial, domestic, agricultural and medical waste waters. Cobalt (II) as one of the most dangerous pollutants is introduced into the water media at remarkable concentrations by various manufactures [3]. In the last several years, environmentalist attention has been attracted considerably on efficient removal of heavy

*Corresponding author.

metals before discharging into the natural environment, because of some characteristics such as bio accumulation and toxicity even in low concentrations. In this regards, several treatment technologies including chemical precipitation, filtration, adsorption, ion exchange, membrane and coagulation-flocculation have been widely applied [4–7]. However, most of them suffer from several draw backs like high energy and chemicals consumption, higher operational and capital costs as well as problems regarding sludge disposal [8,9]. Adsorption process has been introduced as a most applicable and favorable technique for decontamination of waste waters, due to the easy operation, high efficiency at wide range of contaminant concentration, operational feasibility, easily regeneration of applied sorbent and cost-effectiveness [10,11].

During the past few years, a wide number of adsorbents (zeolite, carbon materials, silica, agricultural waste biomass, metal oxides, resins and etc.) has been employed for treatment of Co(II) contaminated-water [3,12]. However, most of these sorbents have low specific surface area and adsorption capacity for removal of metal ions. In contrast, the carbonaceous materials, especially activated carbon (AC), showed satisfactory results for effective removal of heavy metals which is associated with huge surface area, the presence of wide spectrum of surface functional groups, high adsorption capacity, plentiful micro and meso porous and pore texture [13–15]. However, some carbon nano materials including carbon nano tubes and graphene-based composites suffer from several serious operational problems such as difficult and costly synthesis, causing turbidity in effluent and need for centrifuges, which totally restricted their potential in the practical applications [11,15,16].

Lots of researchers have paid high attentions on the application of granular activated carbon (GAC) for removal of metal ions, since it can be separated easily from aqueous media and does not cause turbidity in the treated water, compared to powdered form. However, GAC possess lower surface area, in comparison with the powdered form. To overcome this problem, chemical modification of GAC surface has been reported as an effective approach for enhancement of the adsorption capacity of GAC. In this regards, sodium dodecyl sulfate (SDS), as an anionic surfactant, has been widely applied for enhancement of the adsorption capacity of various adsorbents through changes of surface functional groups, as reported in the literature.

Therefore, the aim of this work is improvement of the adsorption properties of GAC via chemical modification by SDS, for treatment of heavy metal-contaminated aqueous solution. To the best of our knowledge, no study has been carried out on the application of SDS modified GAC (MGAC) for the removal of Co(II) ions from aqueous media. The adsorbent was characterized by using various techniques and its potentials were evaluated for removal of Co(II). The adsorptive performance of MGAC was evaluated as a function of SDS loading, solution pH, contact time, temperature and different concentrations of adsorbent and metal ions by a series of batch adsorption tests. Experimental data were fitted via different equilibrium models. Moreover, the rate kinetics and thermodynamics of the adsorption process was performed.

2. Materials and methods

2.1. Materials and reagents

In this work, analytical reagent-grade chemicals were used without further purification. GAC (1.5 mm extra pure), SDS ($CH_3(CH_2)_{11}SO_4^-Na^+$, > 85 %) and cobalt standard stock solution were purchased from Merck (Darmstadt, Germany). pH of samples was adjusted by adding 0.1 M hydrochloric acid (HCl) and sodium hydroxide (NaOH) solutions. All the reagents were prepared with de-ionized water (DI-water) and kept in a refrigerator at 4°C, prior to experiments. Co(II) solutions with desired concentrations were prepared by diluting the stock solution with DI-water. The concentrations of metal were measured by atomic absorption spectrophotometry (AAS, Analytikjenavario 6, Germany) at wavelength 240.7 nm. All measurements were performed in an air/acetylene flame. The lamp current and slit width were 2.0 mA and 1.2 nm, respectively. The instrumental settings of the manufacturer were followed. The instrument was calibrated with a standard solution within a linear range and a high correlation coefficient ($R^2 > 0.99$) was obtained.

2.2. Modification of GAC by SDS

Herein, GAC modification experiments were conducted at different concentrations of SDS (1-5 mol/L) for varying contact times(1–8 h). First, GAC was washed sequentially with DI-water to improve its purity under room temperature. After filtration, GAC was dried in an oven at 70°C for 24 h and stored in a desiccator under dry conditions for next use. Thereafter, 0.5 g prepared GAC was dissolved in 50 mL SDS solution with a certain concentration. The mixture was stirred by a shaker for an appropriate period of time at a rate of 200 rpm under constant temperature (25 ± 1°C). The solid materials were collected using a What man filter (0.45- μm), washed at least three times with DI-water and then dried at 70°C for 5 h. Finally, modified GAC (MGAC) was stored in a brown sealed bottle under dry conditions for characterization and future use.

2.3. Characterization of adsorbents

The surface and morphological characteristics of GAC and MGAC before and after Co(II) adsorption were analyzed using field emission scanning electron microscopy (FESEM, Mira 3-XMU), at 10 keV. Fourier transform infrared spectroscopy (FTIR) spectra of the samples were obtained using BRUKER's Vertex 70 model to determine the functional groups present on the adsorbents surfaces.

2.4. Adsorption experiments procedure

All experiments were carried out in 250 mL flasks filled with 100 mL Co(II) solution at 250 rpm agitation speed in a batch system. Initially, the effect of different concentrations of SDS in the range of 0.5–5.0 mol/L and modification time ranging 1–8 h on Co(II) ions removal performance by modified GAC was evaluated to determine the best adsorbent with maximum efficiency. Afterwards, batch adsorption experiments were performed as a function of solution pH

(2.0–8.0), adsorbent dosage (0.4–1.5 g/L), agitation speed (100–400 rpm), initial Co(II) concentrations (20–100 mg/L), contact time and temperature (25–40°C). Therein, pH of samples was adjusted using 0.1 M HCl and 0.1 M NaOH solutions and then a certain amount of adsorbent was put in the aqueous solution having a fixed concentration of metal ions. The flasks were agitated well for a known period of time to reach adsorption equilibrium conditions. During experiments, at defined time intervals, 2 mL of the solution was periodically taken from each flask and then the samples were subjected to solid-liquid separation. Thereafter, the residual concentration of Co(II) ions in the solution was measured according to the ASTM using a AAS instrument [17]. The adsorption capacity of MGAC for the Co(II), q_e (mg/g), and the removal efficiency were determined using the following equation:

$$\text{Adsorption capacity } (q_e, \text{mg/g}) = \left[\frac{C_0 - C_e}{W}\right] \quad (1)$$

$$\text{Removal efficiency (Re\%)} = \left[\frac{C_0 - C_e}{C_0}\right] \times 100 \quad (2)$$

where C_o and C_e are the initial and equilibrium concentrations of Co(II) (mg/L), W is the ratio of adsorbent quantity to the solution volume (g/L) and q_e is the adsorption capacity (mg/g).

Under above-mentioned conditions, all tests were conducted with three replications and mean values, whose standard deviation never exceeded 5%, were reported as final results. All flasks were rinsed with a 5% HNO_3 solution which was followed by deionized water and then oven-dried. During experiments, a series blanks containing Co(II) solution without the adsorbent was run in parallel and agitated concurrently to establish accuracy, reliability and reproducibility.

2.5. Adsorption kinetics

Kinetic models mainly are employed for evaluation of mechanism of the adsorption process. Kinetic study is important for prediction of the absorbent uptake removal rate from aqueous solutions in order to design an appropriate adsorption unit. In this work, four widely–used adsorption isotherm models (e.g., pseudo-first-order (PFO), pseudo-second-order (PSO), intra particle diffusion (IP), and Elovich) were applied for modeling the adsorption process. The non-linear and line are quations along with constants regarding these kinetic models are presented in Table 1. k_f (1/min) and k_s (mg/g min) are the rate coefficients for PFO and PSO kinetic models, respectively. Also, q_e and q_t (mg/g) are the adsorption capacities at equilibrium and at time t, respectively. As reported in the literature, *IP* model is mostly utilized to understand the adsorption process mechanism. K_{IP} (mg/g $min^{0.5}$) is the rate constant of *IP*, and C_{IP} (mg/g) is the constant depicting the boundary layer effects. For Elovich model, α (mg/g min) and β (g/mg) parameters denote the initial adsorption rate and activation energy for chemical adsorption, respectively.

2.6. Correctness of kinetic models

Herein, the accuracy of kinetic models,apart from correlation coefficient (R^2), was also evaluated via the relationship between the predicted and actual values of q_e, based on adjusted R^2 ($R^2_{ad}j$) and error analysis (F_{error}). The values of R^2, R^2 *adj* and F_{error} (%) were determined using Eqs. (3), (4) and (5), respectively. It was well-known that the higher values of R^2 and R^2_{adj} as well as the smaller F_{error} (%) values suggest the most appropriate model that could be present more accurate estimation of corresponding q_t values.

$$R^2 = \left(\frac{\sum_i^n \left(q_{e,\exp} - \overline{q}_{e,\exp}\right)^2 - \sum_i^n \left(q_{e,\exp} - q_{e,cal}\right)^2}{\sum_i^n \left(q_{e,\exp} - \overline{q}_{e,\exp}\right)}\right) \times 100 \quad (3)$$

$$R^2_{adj} = 1 - (1 - R^2) \cdot \left(\frac{n_p - 1}{n_p - p}\right) \quad (4)$$

$$F_{error}\ (\%) = 100 \times \sqrt{\left(\frac{1}{n_p - p}\right) \cdot \sum_i^n \left(\frac{q_{e,\exp} - q_{e,cal}}{q_{e,\exp}}\right)^2} \quad (5)$$

Table 1
The constants and equations of kinetic and isotherm models studied for Co(II) adsorption onto MGAC

Kinetic/isotherm models	Equation	Linear equation	Plot	Parameters
Kinetic models				
Pseudo-first order	$dq_t/dt = k_1(q_e - q_t)$	$ln(q_e - q_t) = lnq_e - k_1 t$	$ln(q_e - q_t)$ *vs. t*	q_e(mg/g), $k_1(min^{-1})$
Pseudo-second order	$dq_t/dt = k_2(q_e - q_t)^2$	$t/q_t = t/q_e + 1/k_2\, q_e 2$	t/q_t *vs. t*	q_e(mg/g), $k_2(min^{-1})$
Elovich	$q_t = \beta\ ln(\alpha\beta t)$	$q_t = \beta\ ln(\alpha\beta) + \beta\ lnt$	q_t *vs. ln t*	α *(mg/g min)*, β *(g/mg)*
Intra-particle diffusion	$q_t = k_{ip}\ t\ 0.5 + C_{ip}$	$q_t = k_{ip}\ t\ 0.5 + C_{ip}$	q_t *vs. t 0.5*	k_{ip}(mg/g min0.5), C_{ip}(mg/g)
Isotherm models				
Freundlich	$q_e = K_F(C_e)1/n$	$lnq_e = ln\ K_F + n{-}1\ ln\ C_e$	$ln\ q_e$ *vs. ln* C_e	K_F(mg/g(L mg)1/n), n
Langmuir	$q_e = (q_m K_L C_e)/(1 + K_L C_e)$	$C_e/q_e = C_e/q_m + 1/K_L q_m$	(C_e/q_e) *vs.* C_e	q_m(mg/g), K_L(L/mg)
Temkin	$q_e = B_1 ln(K_T C_e)$	$q_e = B_1 ln\ K_T + B_1\ lnC_e$	q_e *vs. ln* C_e	q_m(mg/g), K_T
Redlich-Peterson	$q_e = (A_{RP}C_e)/(1{-}B_{RP}C_e g)$	$ln[(A_{RP}C_e/q_e)^{-1}] = g ln C_e + lnB_{RP}$	$Ln[(A_{RP}C_e/q_e)^{-1}]$*vs. ln* C_e	g, $B_{RP}(l{\cdot}mg^{-1})$, $A_{RP}(l{\cdot}mmol^{-1})$

where $q_{e,cal}$ (mg/g) and $q_{e,exp}$ (mg/g) are the theoretically and experimentally determined q_e, respectively. p is the number of parameters of the fitted model and n_p is the number of tests.

2.7. Adsorption equilibrium isotherms

In adsorption processes, the equilibrium studies is necessary and critical to predict the behavior of pollutant adsorption onto the sorbent surfaces. To this purpose, Langmuir, Freundlich, Temkin and Reddish-Peterson isotherm models were used. The equations and parameters related to equilibrium models are given in Table 1. K_L (L/mg) is an empirical constant of Langmuir model which is related to energy or enthalpy of the adsorption. The parameters K_F and 1/n are constants of the Freundlich model, which denote adsorption capacity and intensity, respectively. Langmuir and Freundlich models describe the homogeneous (single-layer) and heterogeneous (multi-layer) adsorption of the adsorbate onto the adsorbent, respectively. Temkin isotherm model is based on indirect interactions of the adsorbate and the adsorbent. It demonstrates that the heat of the adsorption decreases linearly. Therein, $B_1 = RT/bT$, R is the universal gas constant (8.314 J/mol K), T is the temperature (K) and b T is the Temkin constant related to the heat of the adsorption (J/mol). k_T (L/mg) is the equilibrium binding constant corresponding to the maximum binding energy. Isotherm model of Redlich–Peterson equation consists of both features of Langmuir and Freundlich isotherm models. K_{RP}, a_{RP} and g in the Redlich-Peterson isotherm are model constants. K_{RP} is the solute adsorptivity (L g^{-1}), a_{RP} related to adsorption energy (L mg^{-1}) and g is the heterogeneity constant ($0 < g < 1$) [18–20].

3. Results and discussion

3.1. Characterization of MGAC

The morphological and textural features of GAC and modified GAC, before and after metal ions adsorption, were analyzed using FESEM technique. FESEM images of samples are illustrated in Fig. 1. As observed, the external surface of GAC (Fig. 1a) is more porous than MGAC before using in adsorption process (Fig. 1b). Compared to GAC, the external surface of MGAC is relatively flat and has lower roughness and irregularities. Their regular surface of GAC can be associated with the presence of pores and/or distribution of active sites on its surface. It is noticeable that some pores and the clump cavities still present in the MGAC structure after modification, which could provide more reactive sites as well as high potential for MGAC to adsorb pollutants. However, MGAC surface roughness was decreased significantly after loading Co(II) ions during the adsorption process as shown in Fig. 1c. Decreasing the roughness of MGAC can be attributed to the pore filling by metal ions during the process of adsorption. Results confirmed that Co(II) ions were adsorbed effectively on the MGAC surface and the adsorption process took place in an efficient way.

In order to characterize the functional groups on the surfaces of the samples and to determine the binding mechanism of the pollutants, FTIR spectra of GAC and MGAC, before and after adsorption of metal ions, were prepared in

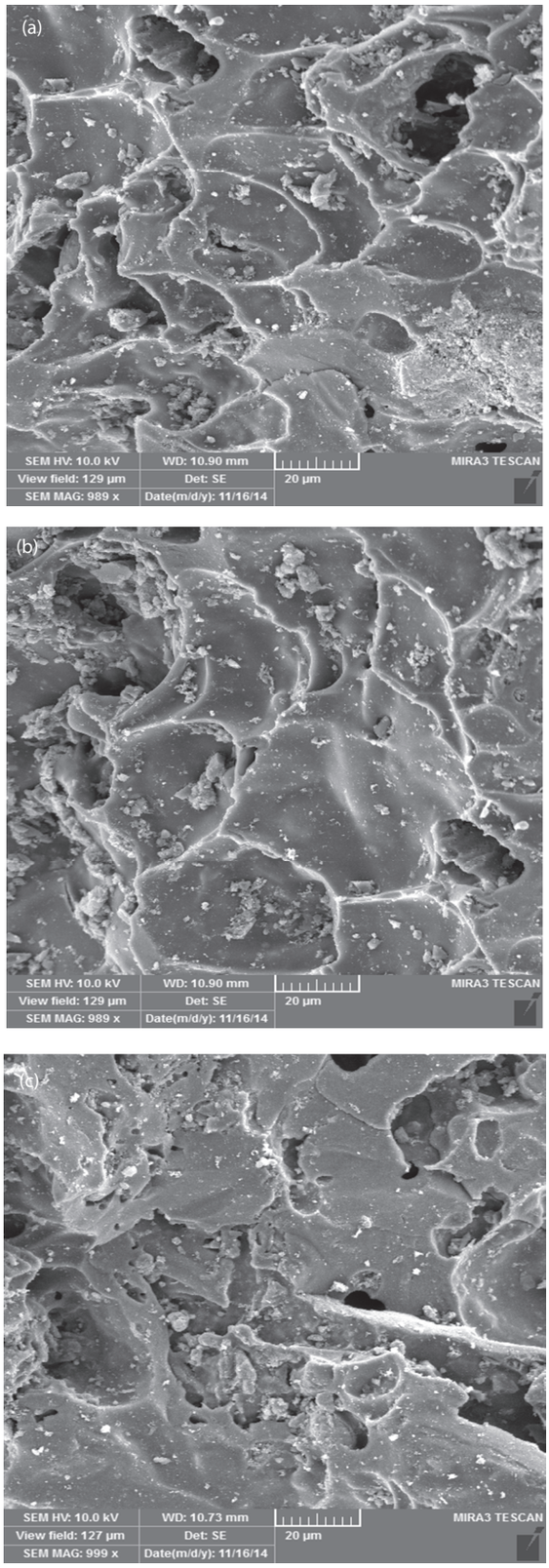

Fig. 1. FESEM images of GAC (a), MGAC (b) and MGAC after Co(II) adsorption (c).

the range of 400–4000 cm^{-1} which are shown in Figs. 2a–c. Results of FTIR analyzes revealed some absorption peaks belonging to various functional groups or different vibration modes. For GAC spectra (Fig. 2a), the broad bonds at 3415 cm^{-1}, 3742 cm^{-1} and 3840 cm^{-1} can be assigned to O–H and N–H bonds stretching [1,21]. The absorption peak at 1695 cm^{-1} was belonged to stretching vibration of C=O bond. The bounds observed in the range of 1690–1760 cm^{-1} indicated the presence of –COOH groups on GAC surface [22]. In addition, the absorption peaks at 1520 cm^{-1} and 1134 cm^{-1} were corresponded to N–O bond and C–O bond, respectively [22]. Almost all peaks related to GAC were also observed with little changes in the spectrum of MGAC before Co(II) adsorption, as shown in Fig. 2b. However, some other peaks were appeared in the spectrum of GAC when it was modified with SDS. The absorption bonds at wave number (ν) values ~2880 and ~1646 cm^{-1} can be attributed to $–CH_2$ and C=C bonds, respectively. Herein, $–CH_2$ group is due to the alkane groups which comes from SDS [22]. Moreover, the peaks at around 1350–1450 cm^{-1} and 700–900 cm^{-1} can be apportioned to the S=O and S–O–C bonds, respectively. Results clearly certificated that SDS was successfully encapsulated into the GAC structure. For MGAC after Co(II) adsorption (Fig. 2c), functional groups such as $–CH_2$ (1646 cm^{-1}), N–O (1520 cm^{-1}) and C–O (1132 cm^{-1}) were affected by metal ions adsorption. Furthermore, the intensity absorption of peak of 2880 cm^{-1} which assigned to C–H bond was reduced remarkably after adsorption Co(II) ions. As presented in Fig. 2c, the absorption peaks belonged to S=O and S–O–C bonds were not appeared in the MGAC spectra after adsorption process. As compared to GAC spectrum, the absorption peak at 1132 cm^{-1} (attributed to C–O bond) was broader after Co(II) adsorption, indicating that the adsorption of metal ions was affected by these functional groups.

3.2. Effect of SDS concentration

To obtain the maximum adsorption capacity for GAC, it was modified by different concentrations of SDS in the range of 0.5–5.0 mol/L within contact time of 8 h. Fig. 3 exhibits the comparison removal efficiencies of Co(II) ions by GAC and GAC modified by various loadings of SDS. As observed, for all studied concentrations of SDS except 5.0 CMC, the adsorption efficiency of MGAC was higher than that GAC. This means that the adsorptive performance of GAC was improved by modification with SDS. As can be seen from Fig. 3, the removal percentage of metal ion increased with increasing SDS loading from 0.5 to 1.5 CMC, then followed by a significant decrease with further loadings of SDS. So that, the removal rate enhanced from 56.3 to 72.4% when SDS loading on GAC was enhanced from 0.5 to 1.5 CMC, respectively, during 8 h adsorption. However, the adsorption rates were dropped substantially and reached 71 and 0.0 % for 2.0 SDS and 5.0 CMC concentrations, respectively. A possible reason for this phenomenon may be related to the blockage of GAC pores and reduction of surface area of GAC at higher loadings of SDS. From Fig. 2, it is also found that there is not remarkable changes between the adsorption percentage in contact times of 6 and 8 h for SDS of 1.5 CMC, respectively. Therefore, 1.5 CMC and SDS and 6 h contact time were chosen as favorable values for optimum modification of GAC,

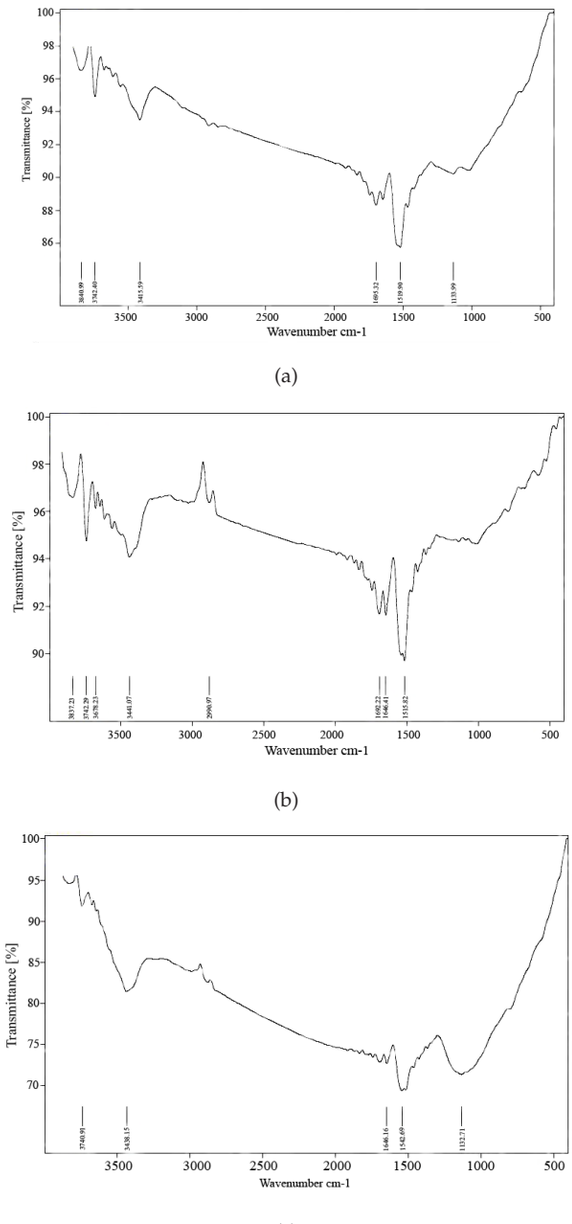

Fig. 2. FTIR spectra of GAC (a) and MGAC before (b) and after (c) adsorption of Co(II) ions.

because of adsorption maximum of Co(II) ions was obtained under these conditions. In the following, this MGAC was applied for all the subsequent adsorption tests.

3.3. Adsorption studies of Co(II)

3.3.1. Effect of solution pH

In adsorption processes, pH of aqueous solution plays an important role,due to the significant effect on solubility and speciation of the metal ions, adsorbate ionization degree, surface charge of the adsorbent as well as functional

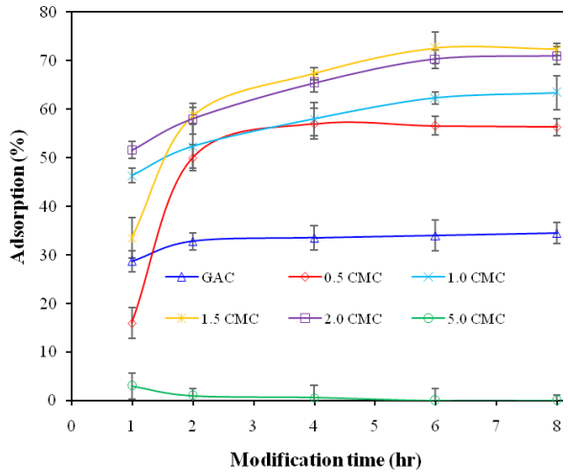

Fig. 3. Effect of various concentration of SDS on the adsorption performance of Co(II) ions by MGAC.

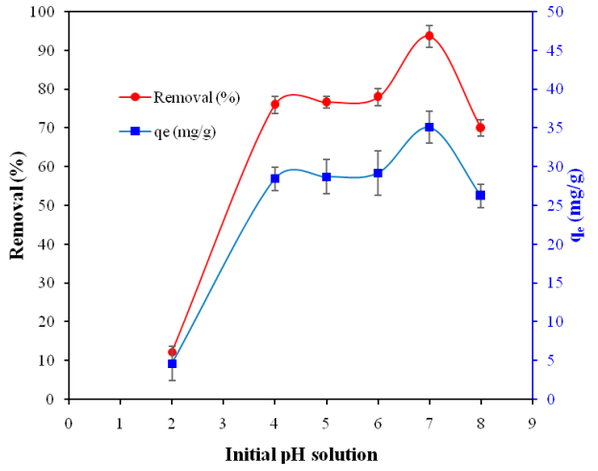

Fig. 4. Effect of initial solution pH on the adsorption capacity and adsorption percentage of Co(II) by MGAC during 60 min (experimental conditions: 1.2 g/L adsorbent, 30 mg/L Co(II), 200 rpm and 20 ± 1°C).

groups of adsorbent [5,23]. Since hydroxide form of metals can be formed at higher pH values, so the study of the influence of solution pH on adsorption process was performed in the range of 2.0–7.0. Hence, the adsorption experiments were carried out successfully without metal precipitation. Fig. 4 shows the effect of initial solution pH on the removal efficiency of Co(II) ions by MGAC. Results illustrate that the adsorption rate of metal ions is highly dependent on the initial pH of solution. So that, the uptake of metal ions was improved from 12.3 to 93.6% as solution pH raised from 2.0 to 7.0, respectively, for 30 mg/L Co(II) concentration and 2 g/L adsorbent during 60 min agitation time. In highly acidic media, low adsorption is associated with the strong competition between protons (H^+) and metal cations (Co(II)) for the adsorption sites, which consequently decreased the adsorption rate [1,24]. Under these conditions, moreover, the surface of the adsorbent is positively charged and so, electrostatic repulsion happens between cations and protons for the adsorption on active sites. On the other hand, decreasing the adsorption rate at strong alkaline conditions can be attributed to the formation of metal hydroxides [14,25]. Therefore, it expected that the maximum adsorption occurred at neutral environments. As seen from Fig. 4, the adsorption of Co(II) ions on MGAC was favored at neutral pH values, which is probably due to the changes of surface properties of both adsorbate and adsorbent. Our results were consistent with those of previous studies for several sorbent-Co(II) sorption processes [26–29]. In the literature, it has been reported that when solution pH enhanced, the number of negatively charged sites was enhanced, accordingly led to the promotion of the attraction forces between heavy metals and these beads surface [30]. Furthermore, Lingamdinne et al., who studied the Cd^{2+} adsorption on graphene oxide demonstrated that the numbers of competing hydrogen ions are lower when pH value is 7.0 and more ligands are exposed with negative charges, resulting in greater Co(II) ions sorption [26]. Therefore, considering the maximum removal of Co(II), pH = 7.0 was selected as an optimal value for further adsorption experiments, which would be able to remove Co from wastewater without pre-adjustment of pH.

3.3.2. The effect of adsorbent dose

Amount of adsorbent as an operating parameter can also affect the performance of adsorption process. The influence of variation of adsorbent dosage on the removal efficiency of Co(II) ions and also adsorption capacity of MGAC is depicted in Fig. 5. As observed, the equilibrium concentration in solution phase was decreased substantially with enhancing the adsorbent quantity, whereas the adsorption capacity was reduced significantly. According to Fig. 5, by raising adsorbent amount from 0.4 to 1.5 g/L, the uptake of metal ions was increased from 51.3 to 95 %, while the adsorption capacity was decreased from 38.5 to 19 mg/g, respectively. It is well known that increasing adsorbent dosage provides the additional active sites and/or greater surface area for the adsorption at a fixed initial solute concentration [1,31]. In case of the adsorption capacity, however, the decrease can be explained by some convincing reasons: i) either the split in the flux or the concentration gradient between solute concentration in the Co(II) concentration in solution and the Co(II) amount in the sorbentsurface, ii) unsaturation and/or lower exploitation of active sites on adsorbent at higher dosages and iii) increasing particle interactions and the formation of aggregates and consequently self-binding of adsorbent particles may reduce the amount of pollutant adsorbed per adsorbent mass unit [20,32,33]. As shown in Fig. 5, the uptake of Co(II) for dosages 1.2 and 1.5 g/L was almost same and no significant difference was observed between them. Thus, we considered the adsorbent dosage 1.2 g/L as an optimum amount for conducting the subsequent tests, because the remarkable change is not observed by further increase.

3.3.3. Effect of contact time

Effect of contact time on the adsorption performance was examined at a period of 4 h under optimum conditions for 30 mg/L Co(II) and results are illustrated in Fig. 6. As can be seen, the adsorption rate of Co(II) on MGAC was ini-

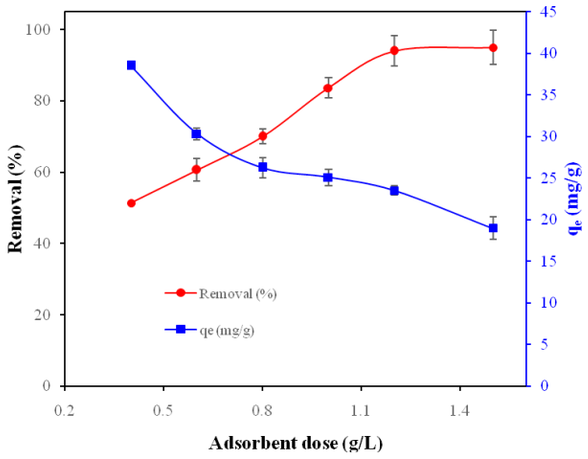

Fig. 5. Effect of different dosages of MGAC on the adsorption capacity and adsorption percentage of Co(II) by MGAC during 60 min (experimental conditions: pH 7.0, 30 mg/L Co(II), 200 rpm and 20 ± 1°C).

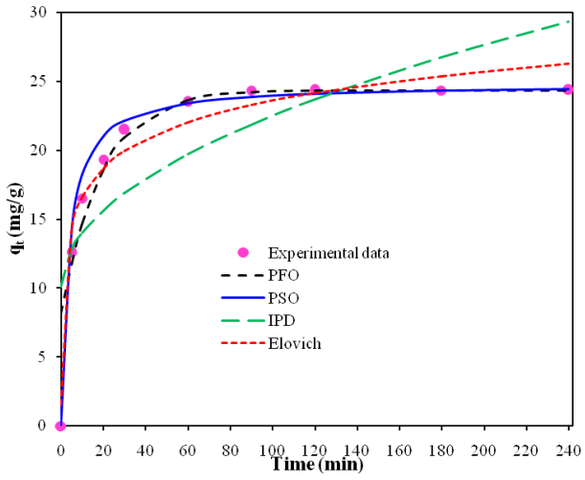

Fig. 6. Effect of contact time and kinetic models of Co(II) adsorption on MGAC (experimental conditions: pH 7.0, 1.2 g/L adsorbent, 30 mg/L Co(II), 200 rpm and 20 ± 1°C).

tially fast and increased rapidly during the first 60 min and then slowed down and reached to equilibrium state after 90 min. It can be noted that the adsorption percentage was improved significantly from 0.0 to 97.4% when contact time reached 180 min, which more than 99% it occurred during the first 90 min. The rapid increase in the adsorption capacity in the initial stages might be associated to the abundance of surface reactive sites that were occupied by the adsorbate molecules. With increasing reaction time, the accessibility of metal ions to unoccupied active sites on the adsorbent surface decreased; and these sites ultimately became saturated when the process reached to equilibrium state. The equilibrium state derived from saturation of the vacant surface reactive sites and diminishing the driving force [10,34]. The equilibrium state is known as a condition that the adsorbate concentration in the aqueous media is in the dynamic balance with the interface. Based on these observations, therefore, 90 min was chosen as an equilibrium time for the future experiments.

3.3.4. Effect of initial Co(II) concentration

In adsorption processes, the adsorbate concentration has a significant role on pollutants adsorption. Effect of different initial pollutant concentrations was evaluated at initial Co(II) concentrations ranging from 20 to 100 mg/L under optimized conditions. Fig. 7 shows the effect of various concentrations of Co(II) on adsorption efficiency and the adsorption capacity. Having a closer look to Fig. 7, it is clear that with increasing the initial Co(II) concentrations, its removal efficiency declined substantially, while the adsorption capacity showed an increasing trend. Results demonstrated that increasing initial concentration of metal ions was unfavorable for enhancing the removal and verified that the adsorption performance was significantly dependent on the concentration of adsorbate. Under these conditions, when initial Co(II) concentration increased from 20 to 100 mg/L, the values of adsorption percentage dropped from 98.2 to 49% and the adsorption capacity raised from 16.4 to 40.8 mg/g, respectively. Decreasing adsorption rate, therein, can be expressed by the fact that at low initial adsorbate concentrations, since the number of vacant surface reactive sites is high, the capability of adsorbent for the adsorption of all adsorbate molecules is high [11,16,35]. Moreover, at higher adsorbate concentrations, all molecules cannot be adsorbed when the number of active sites on the adsorbent is constant, as reported in the literature [13,15]. It was well-known that the ratio of the initial number of adsorbate to the available sorption sites of the adsorbent is decreased at lower initial concentration of adsorbate, and consequently the fractional adsorption of pollutant by the adsorbent becomes independent of its initial concentration. On the other hand, at higher initial concentrations of adsorbate, the available adsorption sites of the adsorbent become fewer and the removal percentage of metal ions is dependent upon the initial concentrations [16,36].

However, the enhancement of adsorption capacity at higher concentrations of adsorbate can be attributed to increasing force of concentration gradient and also improving the interaction between the adsorbent and Co(II) ions. Meanwhile, at higher initial concentrations of adsorbate in the solution, the amounts of adsorbed molecules per unit mass of adsorbent increase effectively. Several authors [23,37] illustrated that the enhancement of both the residual concentration of adsorbate in the aqueous solution and metal ions driving force to facilitate adsorption can propose as most possible reason for the difference between adsorption capacity and removal efficiency affected by initial concentration of metal ions.

3.3.5. Effect of agitation speed

In this study, the influence of agitation speed on the adsorption rate of Co(II) ions onto MGAC was investigated in the range of 100–250 rpm under optimum operational conditions and the results are presented in Fig. 8. As observed, there is no significant change on the adsorption process efficiency for different agitation speeds. Almost, the

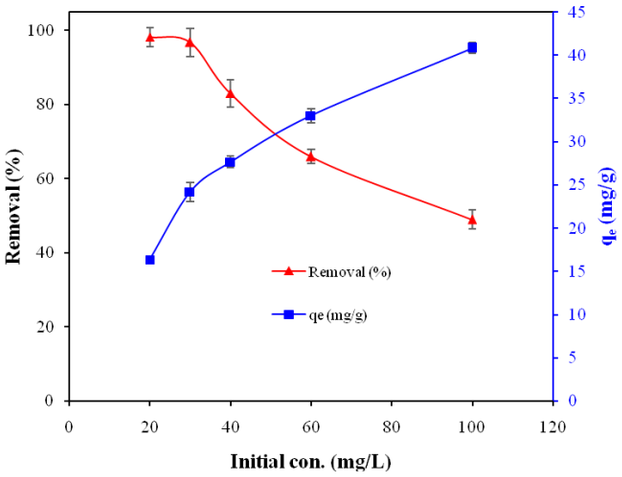

Fig. 7. The changes of the adsorption capacity and removal efficiency regarding the adsorption process of Co(II) on MGAC at various concentrations of metal ions during 90 min (Experimental conditions: pH 7.0, 1.2 g/L adsorbent, 200 rpm and 20 ± 1°C).

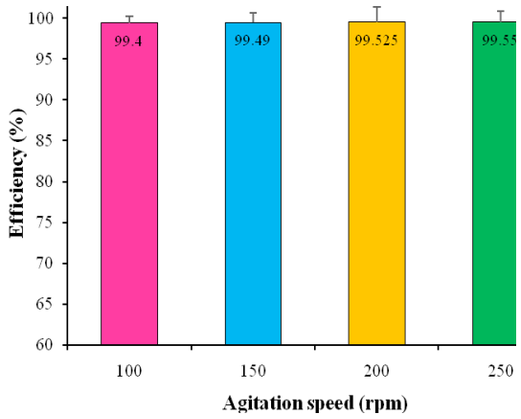

Fig. 8. The changes of the removal efficiency of Co(II) by MGAC as a function of agitation speed within 90 min (experimental conditions: pH 7.0, 1.2 g/L adsorbent, 20 mg/L Co(II) and 20 ± 1°C).

uptake rate of Co(II) ions by MGAC was higher than 99% at all the studied agitation speeds. This means that Co(II) ions adsorption on MGAC is not dependent on the mixing rate. Similar observations have also been reported previously by other researchers for metal ions adsorption on various adsorbents [38].

3.4. Adsorption kinetic studies

The experimental data of study of the effect of contact time provide critical information about the adsorption process kinetics. The values of kinetic models parameters of Co(II) adsorption onto MGAC are listed in Table 2. Herein, the best model was chosen based on the lowest F_{error}, as well as highest amount of R^2_{adj} and R^2. As compared with other models, the highest values of R^2 and R^2_{adj} as well as lowest values of F_{error} were belonged to PSO model, suggesting the highest ability of PSO for describing the adsorption behavior Co(II) ions onto MGAC. Based on the values of R^2, R^2_{adj} and F_{error}, PFO, IP and Elovich kinetic models showed the poor performance to fit the adsorption process as given in Table 2. Furthermore, for PSO model, it is also strongly verified that the calculated q_e value is closer to the experimental q_e value, in comparison with other models, demonstrating this model could better fit the experimental data of Co(II) adsorption, than the other models. The confirmation of this model implies that the rate-limiting step in this adsorption system may be chemisorption involves valences forces thereby electron exchange between the binding sites of the Co(II) ions and MGAC [11,39]. Also, it suggests that the concentrations of both adsorbent and adsorbate are associated with the rate determining step of the adsorption process. Fig. 6 exhibits the fitness of PSO model with studied adsorption process as well as good agreement between plot of PSO model and the experimental data. In the previous conducted studies, the same model showed a very good fit for the adsorption of Co(II) ions on various adsorbents [26,37,40].

Table 2
Parameters of four kinetic models of Co(II) adsorption on MGAC

Kinetic models	Constants	Value
	$q_{e,exp}$ (mg/g)	10.16
Pseudo-first- order		
	$q_{e,cal}$ (mg/g)	16.23
	k_1 (min^{-1})	0.052
	R^2	0.9576
	R^2_{adj}	0.945
	F_{error}	2.89
Pseudo-second-order		
	$q_{e,cal}$	24.8
	k_2 (g/mg)(min)$^{-1}$	0.011
	R^2	0.995
	R^2_{adj}	0.99
	F_{error}	0.91
Intraparticle Diffusion		
	k_{ip} (mg/g min 0.5)	1.24
	C_{ip} (mg/g)	10.1
	R^2	0.6468
	R^2_{adj}	0.635
	F_{error}	4.7
Elovich		
	α	7.85
	β	3.03
	R^2	0.9006
	R^2_{adj}	0.882
	F_{error}	3.42

In adsorption process, the study of IP kinetic model suggested for understand whether the intra-particle diffusion model is the main step in controlling the adsorption process. It was also employed for determination of

the diffusion mechanisms and discerning the plausible rate controlling step which has a significant influence on adsorption kinetics [5,41]. Based on this model, the adsorption rate would be in charge of intra-particle diffusion when the value of intercept of the model equation (C_{ip}) is zero. According to Table 2, the values of C_{ip} was > 0.0, indicating that the intraparticle diffusion is a part of the adsorption, but not the only rate-controlling step in this process. Low correlation coefficient of IP model ($R^2 < 0.7$) also depicts that the adsorption process poorly fits with this model, and pore diffusion was not the rate-limiting step [42]. Hence, it can be stated clearly that the other mechanisms including either complexes or ion-exchange had a significant effect in controlling the adsorptive removal of metal ions on MGAC.

3.5. Adsorption isotherm studies

The equilibrium data provide the critical results to develop adsorption modeling and can be applied as a most paramount factor for designing the adsorption systems. In this work, the adsorption isotherms were evaluated as a function of solution temperature. In this regards, a series tests was performed at different initial concentrations of Co(II) (20–100 mg/L) and various solution temperatures ranging from 20–40°C, when the other operational parameters were set at optimum values. The values and coefficients of related to four studied isotherm models of Co(II) adsorption onto MGAC are summarized in Table 3. Based on comparison between presented R^2 values, Langmuir isotherm model yields a much better fit than the other models in describing the experimental data. According to R^2 values, the adsorption isotherm models fitted the experimental data in accordance to the following order: Langmuir > Freundlich > Redlich-Peterson > Temkin. Fig. 9 also reveals the best fit for Langmuir model with experimental data, implying that this model is better for describing the adsorption process. Similar observations have also been reported previously by other researchers [40,43]. Langmuir model suggests a monolayer sorption with homogeneous functional sites that are distributed uniformly on the surfaces of adsorbent and the adsorption of Co(II) ions onto energetically equivalent sites of the MGAC [44].

The desirability of the adsorption process was also investigated in terms of "R_L", a dimensionless separation factor related to Langmuir model which referred to as an equilibrium parameter ($R_L = (1/(1 + C_0K_L))$). The amount of this factor could vary between zero and one ($0 < R_L > 1.0$), which used to determine the type of adsorption. So that, unfavorable, linear, irreversible and favorable adsorption are assigned to $R_L > 1$, $R_L = 1$, $R_L = 0$ and $0 < R_L < 1$, respectively [45]. Considering this category, the favorable behavior of adsorption of Co(II) ions on MGAC can be confirmed from the values of R_L factor in Table 3, which were obtained between 0 and 1 at both studied temperatures. In addition, the value of $1/n$ (less than unity) in Freundlich isotherm model depicts on the favorable adsorption of Co(II) ions onto MGAC.

In Redlich-Peterson equation, the parameter of 'g' fell in the range of 0 to 1, so that, if 'g' is close to zero Freundlich isotherm, and if it is closer to one the Langmuir isotherm is preferable. Based on the results of Table 3 and the values of 'g' (0.208 and 0.472), it can be concluded that the Freundlich model is preferred. From Table 3, it is noticeable that increasing temperature from 25 to 40°C led to enhancing adsorption capacity of Langmuir model from 27 to 30.1 mg/g. This indicates that the adsorption of Co(II) ions on MGAC is more favorable at higher temperatures, which is in good agreement with results reported in the literature [41,46].

Table 4 shows the monolayer maximum adsorption capacity (q_m) of MGAC and the other adsorbents for the removal Co(II). According to Langmuir isotherm model, the

Table 3
Characteristics of the equilibrium models of adsorption of Co(II) on MGAC under different temperatures

Isotherm models	Temperature (°C)	
	20	40
Langmuir		
Q_m (mg/g)	41.5	51
K_L (L/mg)	0.472	0.616
R^2	0.9903	0.9907
R_L	0.02–0.095	0.016–0.075
Freundlich		
K_F (mg/g(L/mg)$^{1/n}$	21.12	25.5
n	6.21	5.74
R^2	0.9483	0.9767
Temkin		
K_T	152.8	186.57
B_1	4.3	5.21
R^2	0.9382	0.9519
Reddish-Peterson		
g	0.428	0.781
B_{RP} (l·mg^{-1})	11.87	25.9
A_{RP} (l·mmol^{-1})	2.6	2.56
R^2	0.95	0.96

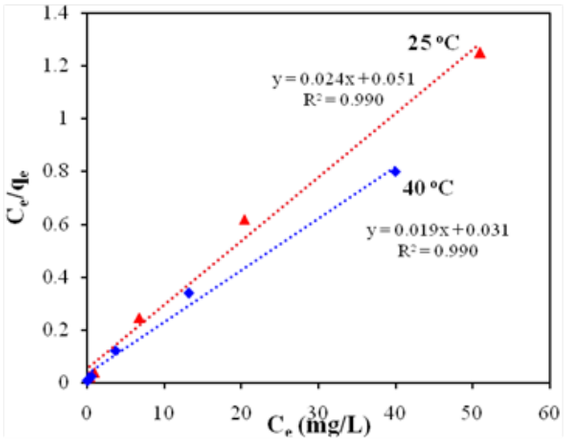

Fig. 9. Accordance of experimental data and Langmuir model for Co(II) adsorption on γ-MGAC at different temperatures (experimental conditions: pH 7.0, 90 min contact time, 1.2 g/L adsorbent, 20–100 mg/L Co(II) and 20–40 ± 1°C).

Table 4
Maximum adsorption capacities of different adsorbents reported in the literature and optimal operational conditions for Co(II) removal

Adsorbent	pH	Isotherm	Kinetic	q_m (mg/g)	References
Graphene oxide	5.5	Freundlich	Pseudo-second-order	21.8	[26]
Natural hemp fibers	5.0	Langmuir	Pseudo-second-order	13.58	[40]
Lemon peel	6.0	–	Pseudo-second-order	22	[42]
Raw rice straw	6.3	Langmuir	Pseudo-second-order	28.5	[46]
Modified rice straw	6.3	Langmuir	Pseudo-second-order	32.3	[46]
Magnetic chitosan nanoparticle	5.5	Langmuir	–	27.4	[47]
Area shell biomass	4.0	Langmuir	Pseudo-second-order	11.53	[48]
Bone char	7.0-8.0	Freundlich	Pseudo-second-order	108.7	[49]
MGAC	7.0	Langmuir	Pseudo-second-order	51	Present work

value of q_m obtained 51 mg/g, which was much greater than that of reported for the other adsorbents. This means that MGAC would be used as one of the efficient adsorbents for the effective adsorption of C_o ions from aqueous solutions. The observed differences in the adsorption capacities for the listed adsorbents can be associated with structural, textural and morphological characteristics, particle size distribution, surface area and the properties of functional groups in each adsorbent. Although some adsorbents showed the q_m values higher than MGAC for Co ions, majority of them have various operational restrictions such as expensive synthesis and preparation. Nevertheless, further studies can be expected to conduct on efficient modification methods of GAC for increasing the surface area and changing functional groups.

3.6. Adsorption thermodynamics

To determine thermodynamic parameters of Co(II) adsorption on MGAC, the effect of solution temperature (25–40°C) on the adsorption efficiency was examined under optimum conditions. The thermodynamic parameters including enthalpy change (ΔH°), entropy change (ΔS°) and Gibbs free energy change (ΔG°) were determined using the following equations:

$$\ln K_L = \frac{\Delta S^o}{R} - \frac{\Delta H^o}{RT} \quad (6)$$

$$\Delta G^o = -RT\ln(K_L) \quad (7)$$

where, R is the gas constant (8.3145 J/mol K), and K_L is the distribution coefficient at temperature T. The values of $\Delta H°$ and $\Delta S°$ were calculated from the slope and intercept of van't Hoff's plots of 1/T versus ln K_L, respectively.

According to the results presented in Table 5, the values of $\Delta H°$, $\Delta S°$ and $\Delta G°$ were positive, positive and negative, respectively. The positive values of $\Delta H°$ also depicted that there was a strong chemical bond between the adsorbate molecules and the external surfaces of adsorbent molecules [46]. The positive values of ΔS^o confirmed an increased randomness at solid-liquid interface during the adsorption process and affinity of the adsorbent for Co(II) ions [37]. An increasing trend in the amount of $\Delta G°$ with increasing temperature indicated that the C_o ions adsorption onto MGAC becomes more favorable at higher temperatures, which is consistent with the results of isotherm studies (Table 3) [42].

Table 5
Thermodynamic parameters of adsorption process of Co(II) on MGAC under optimum conditions

T (K)	298	313
ΔG (kJ/mol)	–2.97	–7.51
ΔS (kJ/mol K)	–0.32	
ΔH (kJ/mol)	28.05	

4. Conclusion

In this work, GAC was modified chemically by SDS to enhance its adsorption capacity for removal of Co(II) ions. The effect of several operational parameters such as solution pH, contact time, adsorbent dosages, initial metal ion concentrations, temperature and agitation speed on the adsorption performance was examined in a batch system. Results depicted that the adsorption ability of GAC was improved significantly after modification, due to synergistic effect. The experimental data were found to be best-fitted with Langmuir isotherm and pseudo-second-order kinetic models. The performance of adsorption process was favorable at neutral pH and higher temperatures. The equilibrium time was also 90 min. In conclusion, the modification of GAC with SDS can be introduced as a promising approach and MGAC can be utilized effectively in the treatment of heavy metal-contaminated waters

Acknowledgement

We are sincerely thankful of Ahvaz Jundishapur University of Medical Sciences for the financial and academic supports of the present research.

Competing interest

We declare no conflict of interest.

References

[1] M. Ahmadi, M. Foladivanda, N. Jaafarzadeh, Z. Ramezani, B. Ramavandi, S. Jorfi, B. Kakavandi, Synthesis of chitosan zero-valent iron nanoparticles-supported for cadmium removal: characterization, optimization and modeling approach, J. Water Supply: Res. Technol.-Aqua, 66 (2017) 116–130.

[2] M. Dardouri, A. ben Hadj Amor, F. Meganem, Preparation, characterization and ion adsorption properties of functionalized polystyrene modified with 1,4-phenylene diisocyanate and diethylenetriamine, Chem. Papers, 69 (2015) 1617–1624.

[3] S. Hashemian, H. Saffari, S. Ragabion, Adsorption of cobalt (II) from aqueous solutions by Fe_3O_4/bentonite nanocomposite, Water Air Soil Pollut., 226 (2015) 1–10.

[4] M.M. Hamed, M. Aly, A. Nayl, Kinetics and thermodynamics studies of cobalt, strontium and caesium sorption on marble from aqueous solution, Chemistry Ecol., (2015) 1–18.

[5] B. Kakavandi, A. Jonidi Jafari, R. Rezaei Kalantary, S. Nasseri, A. Esrafili, A. Gholizadeh, A. Azari, Simultaneous adsorption of lead and aniline onto magnetically recoverable carbon: Optimization, modeling and mechanism, J. Chem. Technol. Biotechnol., 91 (2016) 3000–3010.

[6] M. Harja, G. Buema, D.M. Sutiman, I. Cretescu, Removal of heavy metal ions from aqueous solutions using low-cost sorbents obtained from ash, Chem. Papers, 67 (2013) 497–508.

[7] A.A. Babaei, M. Bahrami, A. Farrokhian Firouzi, A. Ramazanpour Esfahani, L. Alidokht, Adsorption of cadmium onto modified nanosized magnetite: kinetic modeling, isotherm studies, and process optimization, Desal. Water Treat., 56 (2015) 3380–3392.

[8] M. Omidvar Borna, M. Pirsaheb, M. Vosoughi Niri, R. Khosravi Mashizie, B. Kakavandi, M.R. Zare, A. Asadi, Batch and column studies for the adsorption of chromium(VI) on low-cost Hibiscus Cannabinus kenaf, a green adsorbent, J. Taiw. Inst. Chem. Eng., 68 (2016) 80–89.

[9] M. Ahmadi, A.H. Mahvi, Z. Doroud, B. Ramavandi, P. Teymouri, Kinetic and equilibrium studies of nitrate adsorption from aqueous solution by lewatite FO 36, Environ. Eng. Manage. J., 15 (2016) 733–740.

[10] A.A. Babaei, S.N. Alavi, M. Akbarifar, K. Ahmadi, A. Ramazanpour Esfahani, B. Kakavandi, Experimental and modeling study on adsorption of cationic methylene blue dye onto mesoporous biochars prepared from agrowaste, Desal. Water Treat., 57 (2016) 27199–27212.

[11] Majid Kermani, Hasan Izanloo, Roshanak Rezaei Kalantary, Hossein Salehi Barzaki, B. Kakavandi, Study of the performances of low-cost adsorbents extracted from Rosa damascena in aqueous solutions decolorization, Desal. Water Treat., 80 (2017) 357–369.

[12] M. Kara, H. Yuzer, E. Sabah, M. Celik, Adsorption of cobalt from aqueous solutions onto sepiolite, Water Res., 37 (2003) 224–232.

[13] Mehdi Ahmadi, Hasan Rahmani, Bahman Ramavandi, B. Kakavandi, Removal of nitrate from aqueous solution using activated carbon modified with Fenton reagents, Desal. Water Treat., 76 (2017) 265–275.

[14] R. Rezaei Kalantary, A. Jonidi Jafari, B. Kakavandi, S. Nasseri, A. Ameri, A. Esrafili, Simultaneous removal of Lead and Aniline from industrial wastewater using magnetic composite of Fe_3O_4/PAC, Iran Occup. Health J., 12 (2015) 95–110.

[15] A. Jonidi Jafari, R. Rezaei Kalantary, A.A. Babaei, M. Heydari Farsani, B. Kakavandi, Modeling and optimization of adsorption process of reactive dyes on powder activated carbon modified by magnetite nanocrystals, J. Mazandaran Univ. Med. Sci., 26 (2016) 171–187.

[16] A. Azari, A.-A. Babaie, R. Rezaei-Kalantary, A. Esrafili, M. Moazzen, B. Kakavandi, Nitrate removal from aqueous solution by carbon nanotubes magnetized with nano zero-valent iron, J. Mazandaran Univ. Med. Sci., 23 (2014) 15-27.

[17] American Society for Testing and Material (ASTM), Annual book of ASTM, Standard Test Method for Performing the Sieve Analysis of Coal and Designating Coal Size, Method D4749, 2012.

[18] A.A. Babaei, A. Khataee, E. Ahmadpour, M. Sheydaei, B. Kakavandi, Z. Alaee, Optimization of cationic dye adsorption on activated spent tea: Equilibrium, kinetics, thermodynamic and artificial neural network modeling, Korean J. Chem. Eng., 33 (2015) 1352–1361.

[19] A. Behnamfard, M.M. Salarirad, Equilibrium and kinetic studies on free cyanide adsorption from aqueous solution by activated carbon, J. Hazard. Mater., 170 (2009) 127–133.

[20] E.K. Pasandideh, B. Kakavandi, S. Nasseri, A.H. Mahvi, R. Nabizadeh, A. Esrafili, R.R. Kalantary, Silica-coated magnetite nanoparticles core-shell spheres (Fe_3O_4@SiO_2) for natural organic matter removal, J. Environ. Health Sci. Eng., 14 (2016) 1–13.

[21] A. Mohseni-Bandpi, B. Kakavandi, R.R. Kalantary, A. Azari, A. Keramati, Development of a novel magnetite-chitosan composite for the removal of fluoride from drinking water: Adsorption modeling and optimization, RSC Adv., 5 (2015) 73279–73289.

[22] S. Moradi, Microwave assisted preparation of sodium dodecyl sulphate (SDS) modified ordered nanoporous carbon and its adsorption for MB dye, J. Ind. Eng. Chem., 20 (2014) 208–215.

[23] N. Jaafarzadeh, H. Amiri, M. Ahmadi, Factorial experimental design application in modification of volcanic ash as a natural adsorbent with Fenton process for arsenic removal, Environ Technol., 33(1–3) (2012) 159–165.

[24] M. Ahmadi, M. Hazrati Niari, B. Kakavandi, Development of maghemite nanoparticles supported on cross-linked chitosan (γ-Fe_2O_3@CS) as a recoverable mesoporous magnetic composite for effective heavy metals removal, J. Molec. Liq., 248 (2017) 184–196.

[25] A. Azari, B. Kakavandi, R.R. Kalantary, E. Ahmadi, M. Gholami, Z. Torkshavand, M. Azizi, Rapid and efficient magnetically removal of heavy metals by magnetite-activated carbon composite: a statistical design approach, J. Porous. Mater., 22 (2015) 1083–1096.

[26] L.P. Lingamdinne, J.R. Koduru, H. Roh, Y.-L. Choi, Y.-Y. Chang, J.-K. Yang, Adsorption removal of Co(II) from waste-water using graphene oxide, Hydrometallurgy, 165 (2016) 90-96.

[27] E. Erdem, N. Karapinar, R. Donat, The removal of heavy metal cations by natural zeolites, J. Colloid Interf. Sci., 280 (2004) 309–314.

[28] I. Suhasini, G. Sriram, S. Asolekar, G. Sureshkumar, Biosorptive removal and recovery of cobalt from aqueous systems, Process Biochem., 34 (1999) 239–247.

[29] V. Frišták, M. Pipiška, M. Horník, J. Augustín, J. Lesný, Sludge of wastewater treatment plants as Co^{2+} ions sorbent, Chem. Papers, 67 (2013) 265–273.

[30] T. Liu, X. Yang, Z.-L. Wang, X. Yan, Enhanced chitosan beads-supported Fe0-nanoparticles for removal of heavy metals from electroplating wastewater in permeable reactive barriers, Water Res., 47 (2013) 6691–6700.

[31] A.J. Jafari, B. Kakavandi, R.R. Kalantary, H. Gharibi, A. Asadi, A. Azari, A.A. Babaei, A. Takdastan, Application of mesoporous magnetic carbon composite for reactive dyes removal: Process optimization using response surface methodology, Korean J. Chem. Eng., 33 (2016) 2878–2890.

[32] A.A. Babaei, B. Kakavandi, M. Rafiee, F. Kalantarhormizi, I. Purkaram, E. Ahmadi, S. Esmaeili, Comparative treatment of textile wastewater by adsorption, Fenton, UV-Fenton and US-Fenton using magnetic nanoparticles-functionalized carbon (MNPs@C), J. Ind. Eng. Chem., 56 (2017) 163–174.

[33] R. Rezaei Kalantry, A. Jonidi Jafari, A. Esrafili, B. Kakavandi, A. Gholizadeh, A. Azari, Optimization and evaluation of reactive dye adsorption on magnetic composite of activated carbon and iron oxide, Desal. Water Treat., 57 (2016) 6411–6422.

[34] B. Kakavandi, A. Jonidi Jafari, R. Rezaei Kalantary, S. Nasseri, A. Ameri, A. Esrafily, Synthesis and properties of Fe_3O_4-activated carbon magnetic nanoparticles for removal of aniline from aqueous solution: equilibrium, kinetic and thermodynamic studies, Iran J. Environ. Health. Sci. Eng., 10 (2013) 1–9.
[35] M. Ahmadi, B. Kakavandi, S. Jorfi, M. Azizi, Oxidative degradation of aniline and benzotriazole over PAC@FeIIFe2IIIO4: A recyclable catalyst in a heterogeneous photo-Fenton-like system, J. Photochem. Photobiol. A: Chemistry, 336 (2017) 42–53.
[36] R.R. Kalantary, A.J. Jafari, B. Kakavandi, S. Nasseri, A. Ameri, A. Azari, Adsorption and magnetic separation of lead from synthetic wastewater using carbon/iron oxide nanoparticles composite, J. Mazandaran Univ. Med. Sci., 24 172–183.
[37] M. Abbas, S. Kaddour, M. Trari, Kinetic and equilibrium studies of cobalt adsorption on apricot stone activated carbon, J. Ind. Eng. Chem., 20 (2014) 745–751.
[38] B. Kakavandi, R. Rezaei Kalantary, M. Farzadkia, A.H. Mahvi, A. Esrafili, A. Azari, A.R. Yari, A.B. Javid, Enhanced chromium (VI) removal using activated carbon modified by zero valent iron and silver bimetallic nanoparticles, J. Environ. Health Sci. Eng., 12 (2014) 1–10.
[39] A. Takdastan, B. Kakavandi, M. Azizi, M. Golshan, Efficient activation of peroxymonosulfate by using ferroferric oxide supported on carbon/UV/US system: A new approach into catalytic degradation of bisphenol A, Chem. Eng. J., 331 (2018) 729–743.
[40] L. Tofan, C. Teodosiu, C. Paduraru, R. Wenkert, Cobalt (II) removal from aqueous solutions by natural hemp fibers: Batch and fixed-bed column studies, Appl. Surf. Sci., 285 (2013) 33–39.
[41] B. Kakavandi, M. Jahangiri-rad, M. Rafiee, A.R. Esfahani, A.A. Babaei, Development of response surface methodology for optimization of phenol and p-chlorophenol adsorption on magnetic recoverable carbon, Micropor. Mesopor. Maters., 231 (2016) 192–206.
[42] A. Bhatnagar, A.K. Minocha, M. Sillanpää, Adsorptive removal of cobalt from aqueous solution by utilizing lemon peel as biosorbent, Biochem. Eng. J., 48 (2010) 181–186.
[43] A. Ahmadpour, M. Tahmasbi, T.R. Bastami, J.A. Besharati, Rapid removal of cobalt ion from aqueous solutions by almond green hull, J. Hazard. Mater., 166 (2009) 925–930.
[44] S. Jorfi, B. Kakavandi, H.R. Motlagh, M. Ahmadi, N. Jaafarzadeh, A novel combination of oxidative degradation for benzotriazole removal using TiO_2 loaded on FeIIFe2IIIO4@C as an efficient activator of peroxymonosulfate, Appl. Catal. B: Environ., 219 (2017) 216–230.
[45] A. Azari, H. Gharibi, B. Kakavandi, G. Ghanizadeh, A. Javid, A.H. Mahvi, K. Sharafi, T. Khosravia, Magnetic adsorption separation process: an alternative method of mercury extracting from aqueous solution using modified chitosan coated Fe3O4 nanocomposites, J. Chem. Technol. Biotechnol., 92 (2017) 188–200.
[46] A.A. Babaei, Z. Baboli, N. Jaafarzadeh, G. Goudarzi, M. Bahrami, M. Ahmadi, Synthesis, performance, and nonlinear modeling of modified nano-sized magnetite for removal of Cr (VI) from aqueous solutions, Desal. Water Treat., 53(3) (2015) 768–777.
[47] Y.-C. Chang, S.-W. Chang, D.-H. Chen, Magnetic chitosan nanoparticles: Studies on chitosan binding and adsorption of Co(II) ions, React. Funct. Polym., 66 (2006) 335–341.
[48] S. Dahiya, R.M. Tripathi, A.G. Hegde, Biosorption of heavy metals and radionuclide from aqueous solutions by pre-treated arca shell biomass, J. Hazard. Mater., 150 (2008) 376–386.
[49] X. Pan, J. Wang, D. Zhang, Sorption of cobalt to bone char: Kinetics, competitive sorption and mechanism, Desalination, 249 (2009) 609–614.